

Cell Reports Medicine, Volume 5

Supplemental information

**Lymph node and tumor-associated PD-L1⁺
macrophages antagonize dendritic cell vaccines
by suppressing CD8⁺ T cells**

Jenny Sprooten, Isaure Vanmeerbeek, Angeliki Datsi, Jannes Govaerts, Stefan Naulaerts, Raquel S. Laureano, Daniel M. Borràs, Anna Calvet, Vanshika Malviya, Marc Kuballa, Jörg Felsberg, Michael C. Sabel, Marion Rapp, Christiane Knobbe-Thomsen, Peng Liu, Liwei Zhao, Oliver Kepp, Louis Boon, Sabine Tejpar, Jannie Borst, Guido Kroemer, Susan Schlenner, Steven De Vleeschouwer, Rüdiger V. Sorg, and Abhishek D. Garg

SUPPLEMENTARY FIGURES

Lymph node and tumor associated PD-L1⁺ macrophages antagonize dendritic cell vaccines by suppressing CD8⁺ T cells

*Lead contact: abhishek.garg@kuleuven.be

*Correspondence: abhishek.garg@kuleuven.be

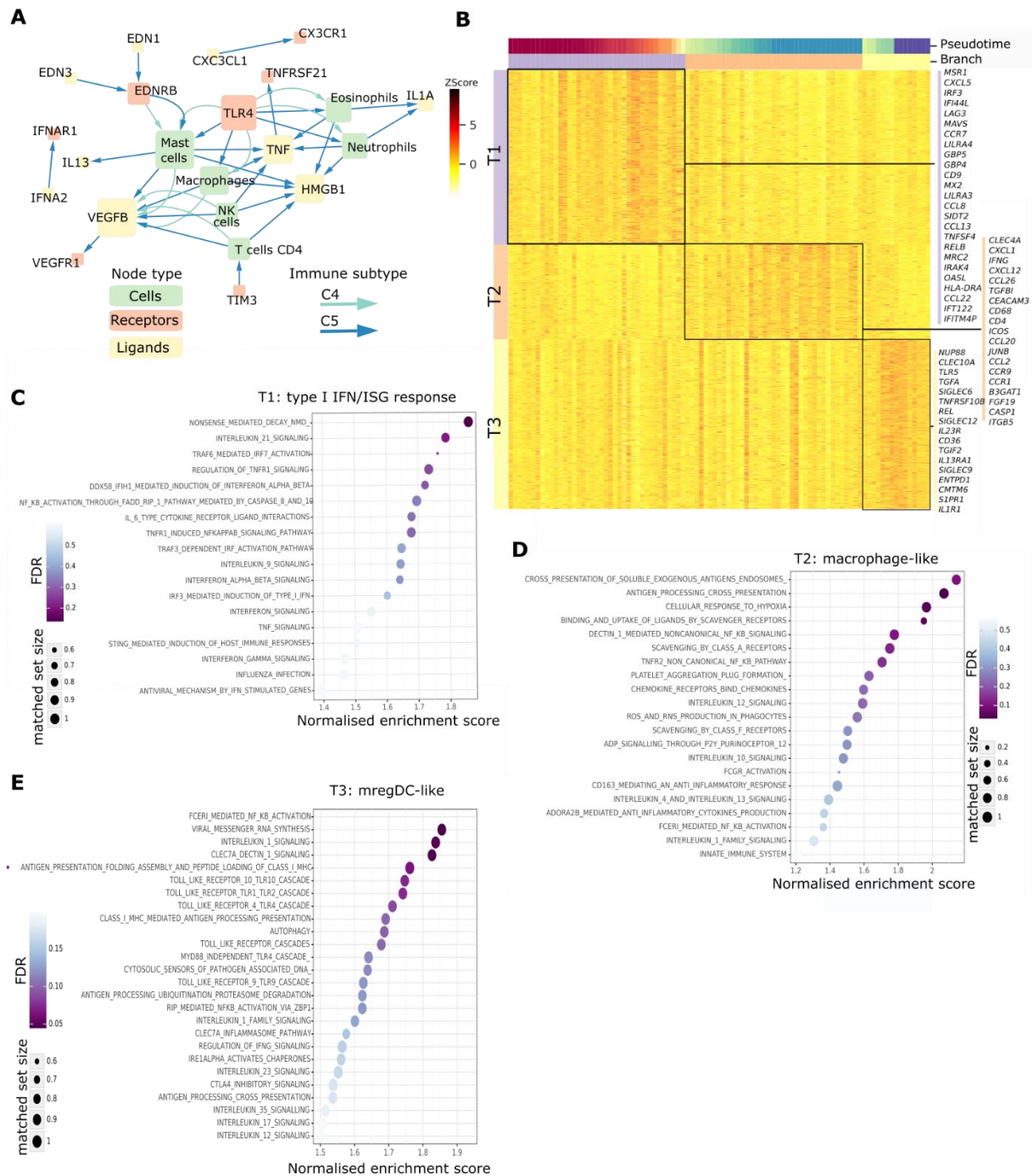


Figure S1, Network and trajectory analysis of humane samples, related to Figure 1.

(A) Discordance or non-correlative extracellular network analysis of the C4/C5 (T cell hostile) human tumors annotated in TCGA pan-cancer dataset (biological replicates; n=224). Of note, in this network, a connection or “pairing” between two nodes (i.e., a pair of two genes or a pair of a gene and an immune cell) indicates that those two nodes are non-correlated to each other thereby indicating discordance of pathway. Node size reflects the number of connections the node participates in (node degree).

(B-E) STREAM DC vaccine trajectory analysis of 93 autologous DC vaccines (biological replicates) pulsed with LPS, IFN γ and TARP peptide generated for 18 prostate adenocarcinoma cancer patients vaccinated with 5-8 vaccines.

(B) Heatmap of upregulated expression per STREAM trajectory branch

(C-E) Gene set enrichment analysis with REACTOME terms per trajectory branch. Dot size corresponds to matched set size and dot color corresponds to FDR (significance: $FDR < 0.05$).

(C) T1: type I IFN/ISG response

(D) T2: macrophage-like.

(E) T3: mature regulatory (mreg) DCs.

Related to figure 1.

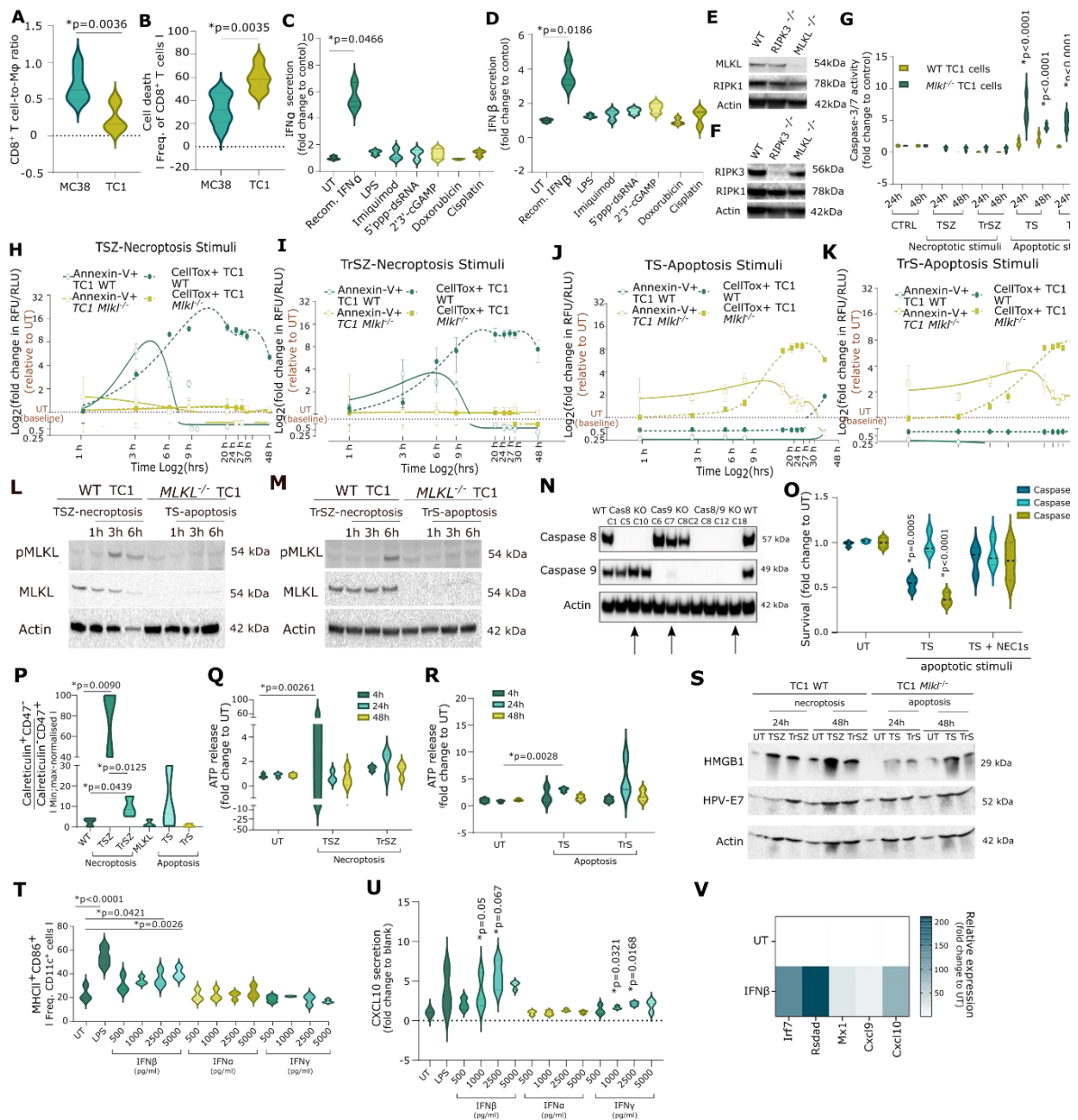


Figure S2, Model optimization of TC1 and MC38 cancer cells to create DC vaccines, related to Figure 2.

(A-B) Violin plots of the flow cytometry analysis of CD45⁺ cell fraction obtained from subcutaneous MC38 and wild-type TC1 tumors on day 23 after tumor cell injection showing (A) CD8⁺ T cell-to-macrophage ratio and (B) percentage of zombie aqua⁺ death/dying in CD8⁺ T cells. (biological replicates; n=6; two-tailed student's t test)

(C-D) Secretion of interferon by wild-type TC1 stimulated with different stimuli for 24h. (C) for IFN α . (D) IFN β . P-values depict comparison to untreated. (biological replicates; n=3; one-way ANOVA, Kruskal-Wallis test).

(E-F) Western blot of wild-type, *Ripk3*^{-/-} and *MLKL*^{-/-} TC1 for MLKL, RIPK1, RIPK3 and Actin.

(G) Caspase 3/7 activity of wild-type and *Mkl1*^{-/-} TC1 stimulated with necroptotic and apoptotic stimuli. P-values depict comparison to 24h or 48h untreated. (biological replicates; n=3; 2way ANOVA, Dunnett's multiple comparisons test).

(H-K) Kinetics of Annexin-V and CellTox staining at different timepoints for dying wild-type and *MLKL*^{-/-} TC1 cells treated with (H) TSZ-necroptotic stimuli (I) TrSZ-necroptotic stimuli (J) TS-apoptotic stimuli (K) TrS-apoptotic stimuli TrS. (biological replicates; n=3).

(L-M) Western blot for phosphorylated MLKL (pMLKL), MLKL and Actin of wild-type and *MLKL*^{-/-} TC1 cells stimulated with necroptotic stimuli and apoptotic stimuli.

(N) Western blot of caspase 8, caspase 9 and actin of different clones of TC1 *Caspase 8*^{-/-}, *Caspase 9*^{-/-} and *Caspase8/9*^{-/-}. Arrows indicate the used clone.

(O) Survival of TC1 *Caspase 8*^{-/-}, *Caspase 9*^{-/-} and *Caspase8/9*^{-/-} stimulated with cell death cocktails. P-values depict comparison to untreated. (n=3; two-way ANOVA, Dunnett's multiple comparisons test)

(P) Calreticulin⁺ CD47⁻-to- Calreticulin⁻ CD47⁺ ratio of wild-type and *Mkl1*^{-/-} TC1 cells treated with necroptotic and apoptotic stimuli. P-values depict comparison to untreated. (biological replicates; n=3; two-tailed student's t test).

(Q-R) ATP release at 4h, 24h and 48h of wild-type and *Mkl1*^{-/-} TC1 cells treated with necroptotic (Q) and apoptotic (R) stimuli. P-values depict comparison to 4h, 24h or 48h untreated. (biological replicates; n=3; one-way ANOVA, Dunnett's multiple comparison test).

(S) Western blot for HMGB1 and HPV-E7 antigen secretion in the media of wild-type and *Mkl1*^{-/-} TC1 cells treated with necroptotic and apoptotic stimuli.

(T) MHCII⁺CD86⁺ of CD11c⁺ of DCs treated with different concentrations of IFN $\alpha/\beta/\gamma$.

(U) CXCL10 secretion of DCs treated with different concentrations of IFN $\alpha/\beta/\gamma$.

(T-U) P-values depict comparison to untreated. (biological replicates; n=3; one-way ANOVA, Dunnett's multiple comparison test)

(V) Relative expression of different interferon-stimulated genes, interferon-response factor 7 (*Irf7*), Radical S-Adenosyl Methionine (*Rsad*), MX Dynamin Like GTPase 1 (*Mxl1*), Chemokine (C-X-C motif) ligand 9 (*Cxcl9*), Chemokine (C-X-C motif) ligand 10 (*Cxcl10*), of which the IFN-signature is composed.

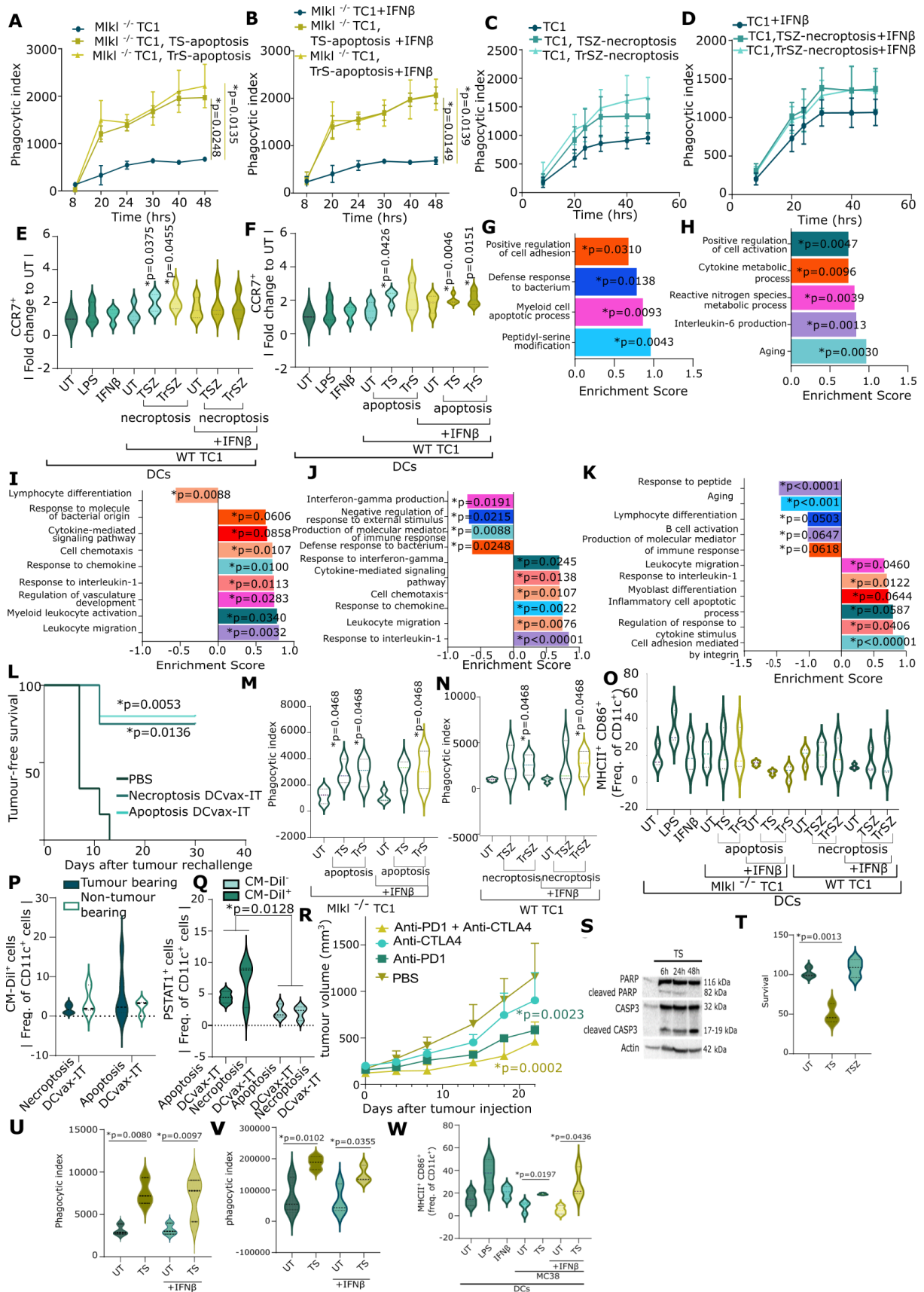


Figure S3, DCvax-it characterization, related to Figure 2 and 3.

(A-D) Efferocytosis index of DCs stimulated with pHRodo stained TC1 cancer cells calculated by the fluorescent intensity values, subtracted by the appropriate 4°C negative control.

(A-B) DCs stimulated with apoptotic *Mkl1*^{-/-} TC1 cells. P-values depict comparison to untreated *Mkl1*^{-/-}TC1 cells or *Mkl1*^{-/-}TC1 cells + IFN β . (biological replicates; n=3; area under curve; one-way ANOVA, Dunnett's multiple comparison test).

(C-D) DCs stimulated with necroptotic wild-type TC1 cells. P-values depict comparison to untreated wild-type TC1 cells. (biological replicates; n=4; area under curve; one-way ANOVA, Dunnett's multiple comparison test).

(E-F) Fold change of mean fluorescence intensity of CCR7 of CD11c⁺ cells to untreated DCs. DCs were stimulated with (E) necroptotic wild-type TC1 cells (F) apoptotic *Mkl1*^{-/-} TC1 cancer cells with and without IFN β . P-values depict comparison to untreated DCs. (biological replicates; n=4 (ts; n=3); one sample t-test).

(G-K) Set enrichment analysis of Gene Ontology Biological Process terms based on the secretome of DCs stimulated with (G) necroptotic wild-type TC1 cells, (H) apoptotic *Mkl1*^{-/-} TC1 cells, (I) untreated wild-type or *Mkl1*^{-/-} TC1 cells with IFN β , (J) necroptotic wild-type TC1 cells with IFN β or (K) apoptotic *Mkl1*^{-/-} TC1 cells with IFN β . P-values < 0.05 are marked with *.

(L) Rechallenge with wild-type TC1 injection after vaccination with necroptosis DCvax-IT, Apoptosis DCvax-IT wild-type DC vaccines. (biological replicates; PBS, n=6; Apoptosis DCvax-IT, n=5; Necroptosis DCvax-IT, n=4, Log-rank (Mantel-Cox) test)

(M-N) Efferocytosis index of *Ifnar1*^{-/-} DCs stimulated with pHRodo stained (M) apoptotic *Mkl1*^{-/-} TC1 cells or (N) necroptotic wild-type TC1 cells. Values were calculated by the fluorescence intensity values, subtracted by the appropriate 4°C negative control (biological replicates; n=3; one-way ANOVA, Kruskal-Wallis test).

(O) Maturation of DCs, assessed by MHCII⁺CD86⁺, untreated or treated with LPS, IFN β or dying cancer cells with or without IFN β (n=3; One-way ANOVA, Dunnett's multiple comparison).

(P) Frequency of Celltracker CM-Dil⁺ CD11c⁺ cells in the lymph nodes of TC-1 tumor bearing and non-tumor bearing mice vaccinated with DCvax-IT. (biological replicates; Tumor bearing, n=6; Non-tumor bearing, n=3; 2-way ANOVA) (This experiment overlapped with experiment in Fig 3G and hence "Tumor bearing" values are identical)

(Q) Frequency of phosphorylated STAT1 (pSTAT1)⁺ in Celltracker CM-Dil⁺ CD11c⁺ and in Celltracker CM-Dil⁺ CD11c^{-NEGATIVE} cells in the lymph nodes of DCvax-IT vaccinated mice. (biological replicates; n=3; 2-way ANOVA)

(R) Tumor volume curve of MC38 tumor-bearing mice treated with anti-PD1 ICB and/or anti-CTLA4 ICB on day 10, 13 and 17 after MC38 injection. (biological replicates; PBS, n=9; anti-CTLA4 ICB, n=4; anti-PD1 ICB, n=4; anti-CTLA4+anti-PD1 ICB, n=4; statistics on area under curve with one-way ANOVA, Dunnett's multiple comparison)

(S) Western blot for PARP, Caspase3 and Actin of MC38 treated with apoptotic stimuli.

(T) Survival of MC38 stimulated with apoptotic (TS) or necroptotic (TSZ) stimuli measured with the MTT assay. P-values depict comparison to untreated MC38 cells. (biological replicates; n=3; One-way ANOVA, Dunnett's multiple comparison).

(U-V) Efferocytosis index of DCs stimulated with pHRodo stained apoptotic MC38 cells with or without IFN β at (U) 24h (V) 48h. Values were calculated by the fluorescent intensity values, subtracted by the appropriate 4°C negative control. P-values depict comparison to untreated or IFN β treated MC38 cells. (biological replicates; n=3; One-way ANOVA, FDR correction according to Benjamini, Krieger and Yekutieli method).

(W) Frequency of MHCII⁺CD86⁺ of CD11c⁺ in DCs stimulated with untreated or apoptotic MC38 with or without IFN β . P-values depict comparison to DCs with untreated or IFN β treated MC38 cells. (biological replicates; n=3; two-tailed student's t test)

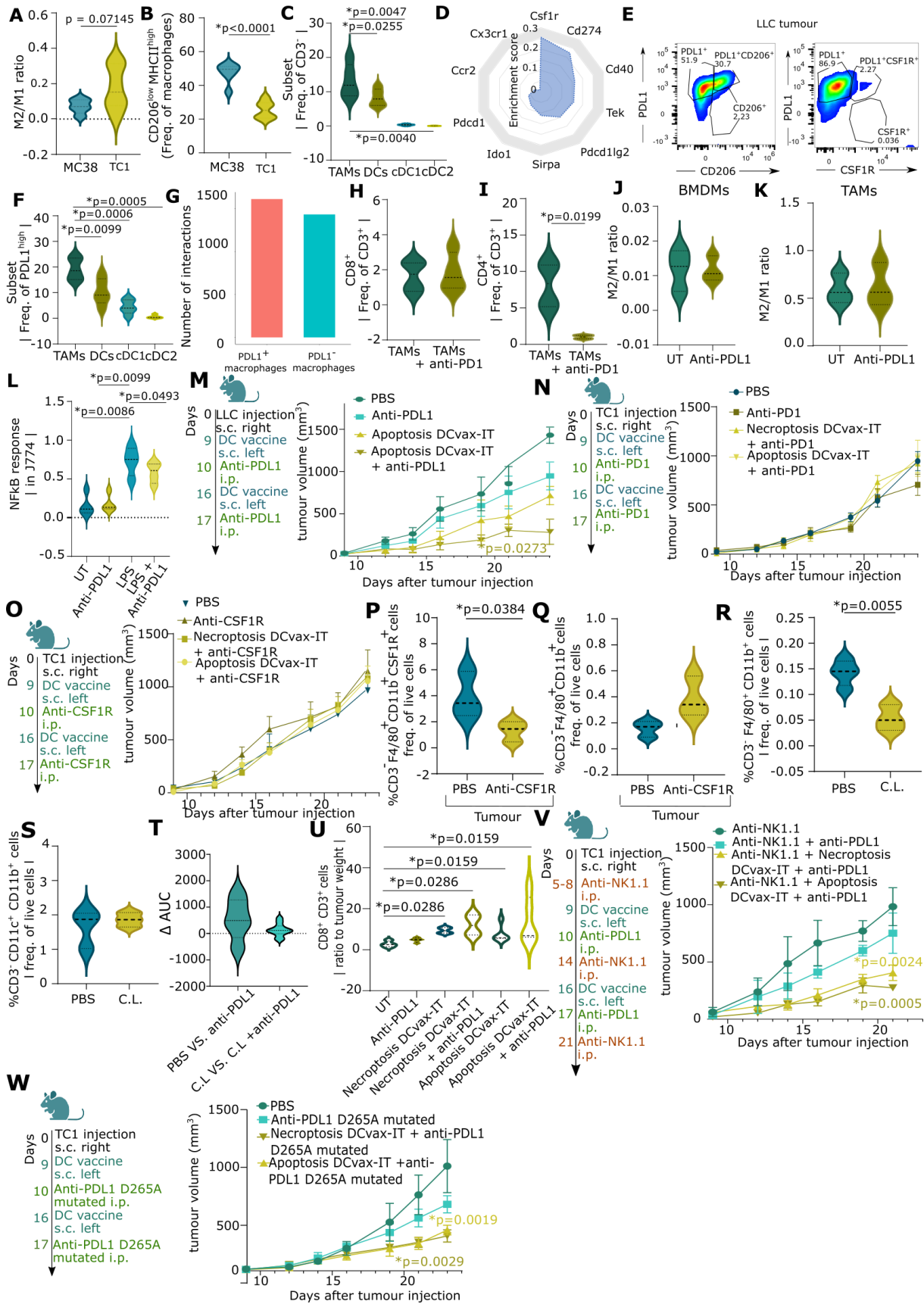


Figure S4, Delineating macrophage phenotypes coupled to DC vaccination, related to Figure 4 and 5.

(A-B) Violin plots of the CD45⁺ cell fraction obtained from subcutaneous MC38 and TC1 tumors on day 23 after tumor cell injection.

(A) M2/M1 ratio present in MC38 and wild-type TC1 tumors (biological replicates; TC1; n=5, MC38; n=6; two-tailed student's t test)

(B) Frequency of CD206^{low} MHCII^{high} cells of CD11b⁺ F4/80⁺ (biological replicates; n=6; two-tailed student's t test)

(C) Frequency of subset of CD3⁻ cells in CD45⁺ cells isolated from wild-type TC1 tumors on day 23 after wild-type TC1 cell injection. Cell populations were assessed by CD11b⁺ F4/80⁺ (TAMs), CD11b⁺CD11c⁺ (DCs), CD11b⁺CD11c⁺XCR1⁺ (cDC1), CD11b⁺CD11c⁺CD172a⁺ (cDC2). P-values depict comparison to TAMs. (biological replicates; n=5; One-way ANOVA, FDR correction according to Benjamini, Krieger and Yekutieli method).

(D) Radar plot illustrating enrichment scores of indicated genes compared to a reference macrophage transcriptomic profile (see materials & methods for more details on computational approach).

(E) Contour plots of flow cytometry analysis of PDL1⁺, CSF1R⁺ and CD206⁺ (gating based on unstained samples) on TAM derived from wild-type LLC tumors isolated on day 23 after tumor cell injection.

(F) Frequency of subset of PDL1⁺ cells in CD45⁺ cells isolated from wild-type TC1 tumors on day 23 after wild-type TC1 cell injection. Cell populations were assessed by CD11b⁺ F4/80⁺ (TAMs), CD11b⁺CD11c⁺ (DCs), CD11b⁺CD11c⁺XCR1⁺ (cDC1), CD11b⁺CD11c⁺CD172a⁺ (cDC2). P-values depict comparison to TAMs. (biological replicates; n=5; One-way ANOVA, FDR correction according to Benjamini, Krieger and Yekutieli method).

(G) Number of interactions of PD-L1/*Cd274*⁺ and PD-L1/*Cd274*⁻ macrophages based on Cellchat algorithm analysis of single-cell (sc)-RNAseq data of TC1-tumours obtained from the existing dataset GSM7103827.

(H-I) Coculture experiments of T cells with wild-type TC1 tumor derived TAMs on day 23 after wild-type TC1 cell injection pretreated for 48h with or without anti-PD1. Frequency of (H) CD8⁺ of CD3⁺ cells (I) or CD4⁺ of CD3⁺ cells. (biological replicates; n=4, two-tailed paired t-test)

(J-K) MHCII^{low} CD206^{high}/CD206^{low} MHCII^{high} (M2/M1) ratio with and without anti-PDL1 treatment for 48h of (J) bone marrow derived macrophages (BMDMs) (K) wild-type TC1 derived TAMs. (biological replicates; n=3; two-tailed paired t-test)

(L) NF-κB response of J774 macrophage genetic reporter cells treated with LPS, anti-PD-L1 ICB or LPS + anti-PD-L1 ICB (biological replicates; n=4; one-way ANOVA, Dunnett's multiple comparison test)

(M) Tumor volume curve of LLC tumor bearing mice treated with DCvax-IT on day 9 and 16 in combination with anti-PDL1 ICB on day 10 and 17. P-values depict comparison to PBS treated mice (biological replicates; n=3-4; statistics based on area under curve, one-way ANOVA, Kruskal-Wallis test).

(N-O) Tumor volume curve of wild-type TC1 tumor bearing mice treated with DCvax-IT on day 9 and 16 in combination with (N) anti-PD1 on day 10 and 17 (O) anti-CSF1R on day 10 and 17. P-values depict comparison to PBS treated mice (biological replicates; n=4-8; area under curve, one-way ANOVA, Dunnett's multiple comparison test).

(P-Q) Violin plots of the CD45⁺ cell population of wild-type TC1 tumors isolated on day 23 after wild-type TC1 cell injection. TC1 tumors were treated with DCvax-IT on day 9 and 16 in combination with anti-CSF1R on day 10 and 17.

(P) Frequency of CD3⁻F4/80⁺CD11b⁺CSF1R⁺ of live cells (biological replicates; n=3; one-tailed student's t test).

(Q) Frequency of CD3⁻F4/80⁺CD11b⁺ of live cells (biological replicates; n=3; two-tailed student's t test).

(R-S) Violin plots of splenocytes of mice treated with clodronate liposomes on day -2,0,2,5,7,9,12,15,17,20,22. Frequency of (R) CD11b⁺ F4/80⁺ of live or (S) CD11b⁺ CD11c⁺ of live (biological replicates; n=3-4; two-tailed student's t test).

(T) Differential analysis of tumor volume curve of wild-type TC1 tumor bearing mice treated with DCvax-IT on day 9 and 16 and/or anti-PD-L1 ICB on day 10 and 17 alone and in combination with clodronate liposomes (C.L.). The figure shows the delta area under the curve (AUC) Values of anti-PD-L1 ICB compared to their respective controls as indicated in the figure. (biological replicates; PBS vs anti-PD-L1 ICB, n=5; C.L. vs anti-PD-L1 ICB + C.L., n=11; Mann-Whitney test)

(U) Frequency of CD8⁺ of CD3⁺ cell (normalized to tumor weight) of CD45⁺ fraction of wild-type TC1 tumors treated with clodronate liposomes on day -2,0,2,5,7,9,12,15,17,20,22, anti-PDL1 on day 10 and 17 and with DCvax-IT on day 9 and 16 isolated on day 23 after wild-type TC1 cells injection. P-values depict comparison to clodronate liposome treated mice (biological replicates; n=4-5; Mann-Whitney test).

(V) Tumor volume curve of wild-type TC1 tumor bearing mice treated with DCvax-IT on day 9 and 16 in combination with anti-PDL1 ICB on day 10 and 17 and anti-NK1.1 antibody on day 5, 8, 14 and 21. P-values depict comparison to PBS treated mice (biological replicates; n=4; statistics on area under curve, one-way ANOVA, Dunnett's multiple comparison test).

(W) Tumor volume curve of wild-type TC1 tumor bearing mice treated with DCvax-IT on day 9 and 16 in combination with anti-PDL1 ICB with D265A mutation on day 10 and 17. P-values depict comparison to PBS treated mice (biological replicates; n=4; statistics on area under curve, one-way ANOVA, Dunnett's multiple comparison test).

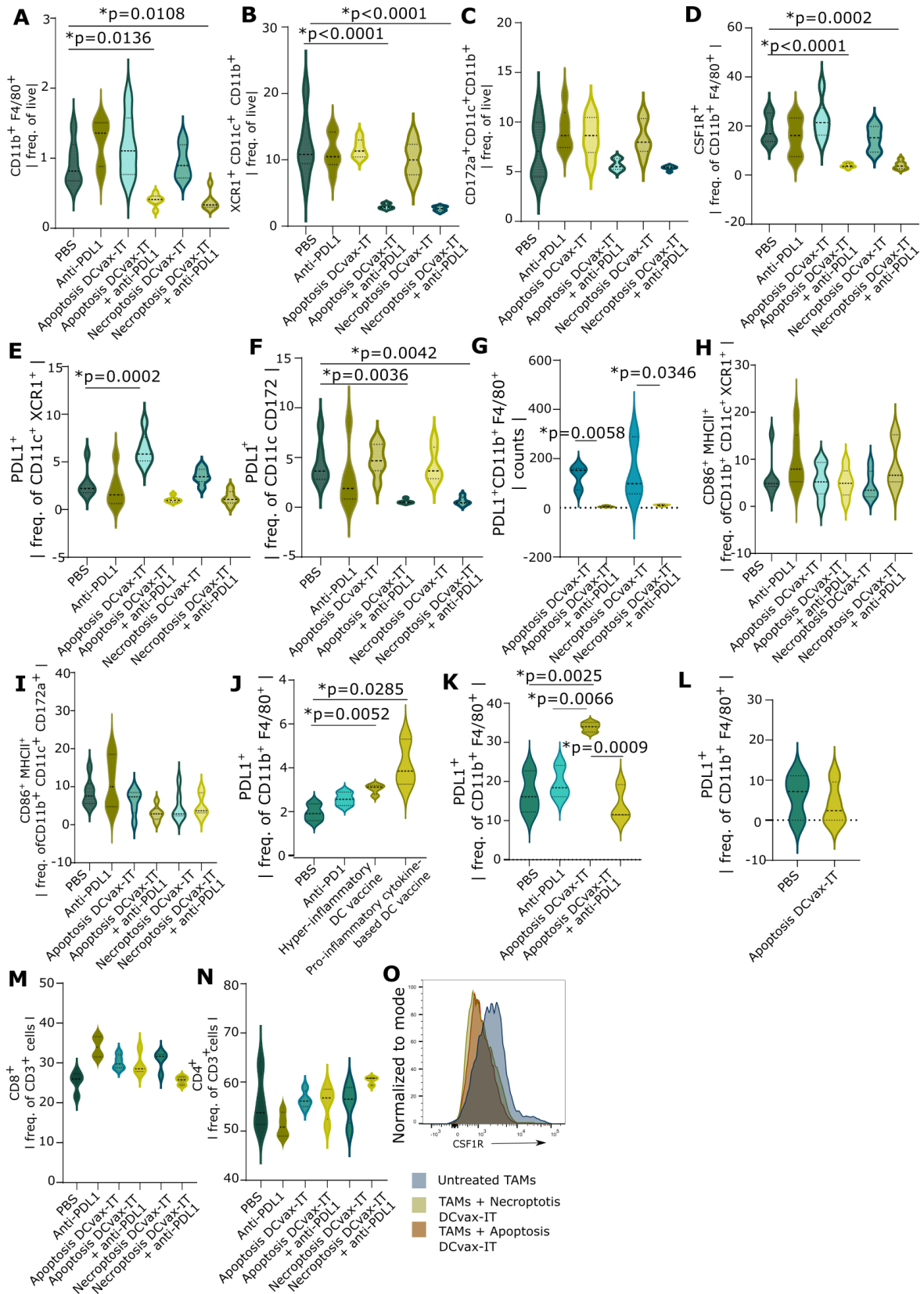


Figure S5, Phenotyping of the lymph nodes of DC vaccinated mice, related to Figure 5.

(A-F) Lymph node analysis of wild-type TC1 tumor-bearing mice treated with DCvax-IT on day 9 with anti-PDL1 on day 10, isolated on day 12. Frequency of (A) $CD11b^+ F4/80^+$ of live (B) $CD11b^+ CD11c^+ XCR1^+$ of live (C) $CD11b^+ CD11c^+ CD172a^+$ of live (D) $CSF1R^+$ of $CD11b^+ F4/80^+$ (E) $PDL1^+$ of $CD11b^+ CD11c^+ XCR1^+$

(F) PDL1⁺ of CD11b⁺ CD11c⁺ CD172a⁺. p-values depict comparison to PBS treated mice (biological replicates; n=5-6; One-way ANOVA, Dunnett's multiple comparisons test).

(G) Lymph node analysis of wild-type TC1 tumor-bearing mice treated with DCvax-IT on day 9 and with anti-PDL1 ICB on day 10, isolated on day 12. Violin plot of absolute counts of PDL1⁺CD11b⁺ F4/80⁺ cells. (biological replicates; n=3-4; one-tailed unpaired t-test)

(H-I) Lymph node analysis of wild-type TC1 tumor-bearing mice treated with DCvax-IT on day 9 with anti-PDL1 on day 10, isolated on day 12. Frequency of (H) MHCII⁺CD86⁺ of CD11b⁺ CD11c⁺ XCR1⁺ (I) MHCII⁺CD86⁺ of CD11b⁺ CD11c⁺ CD172a⁺. p-values depict comparison to PBS treated mice (biological replicates; n=5-6; One-way ANOVA, Dunnett's multiple comparisons test).

(J) Lymph node analysis of wild-type TC1 tumor-bearing mice treated with hyper-inflammatory DC vaccine or pro-inflammatory cytokine-based DC vaccine on day 9 or with anti-PD1 ICB on day 10, isolated on day 12. (biological replicates; n=3-4; unpaired t test)

(K) Lymph node analysis of wild-type LLC tumor-bearing mice treated with DCvax-IT on day 9 and with anti-PDL1 ICB on day 10, isolated on day 12. Violin plot of frequency of PDL1⁺CD11b⁺ F4/80⁺ cells. (biological replicates; n=3; One-way ANOVA, Dunnett's multiple comparisons test)

(L) Lymph node analysis of wild-type MC38 tumor-bearing mice treated with DCvax-IT on day 9, isolated on day 12. Violin plot of frequency of PDL1⁺CD11b⁺ F4/80⁺ cells. (biological replicates; n=3-4; Mann-Whitney test)

(M-N) Lymph node analysis of wild-type TC1 tumor-bearing mice treated with treated with DCvax-IT on day 9 and with anti-PDL1 on day 10, isolated on day 12. Frequency of (M) CD8⁺ of CD3⁺ cells (N) CD4⁺ of CD3⁺ cells. P-values depict comparison to PBS treated mice (biological replicates; n=3-4; One-way ANOVA, Dunnett's multiple comparisons test).

(O) Histogram of CSF1R on CD11b⁺ F4/80⁺ cells of wild-type TC1-derived TAMs-DCvax-IT cocultures.

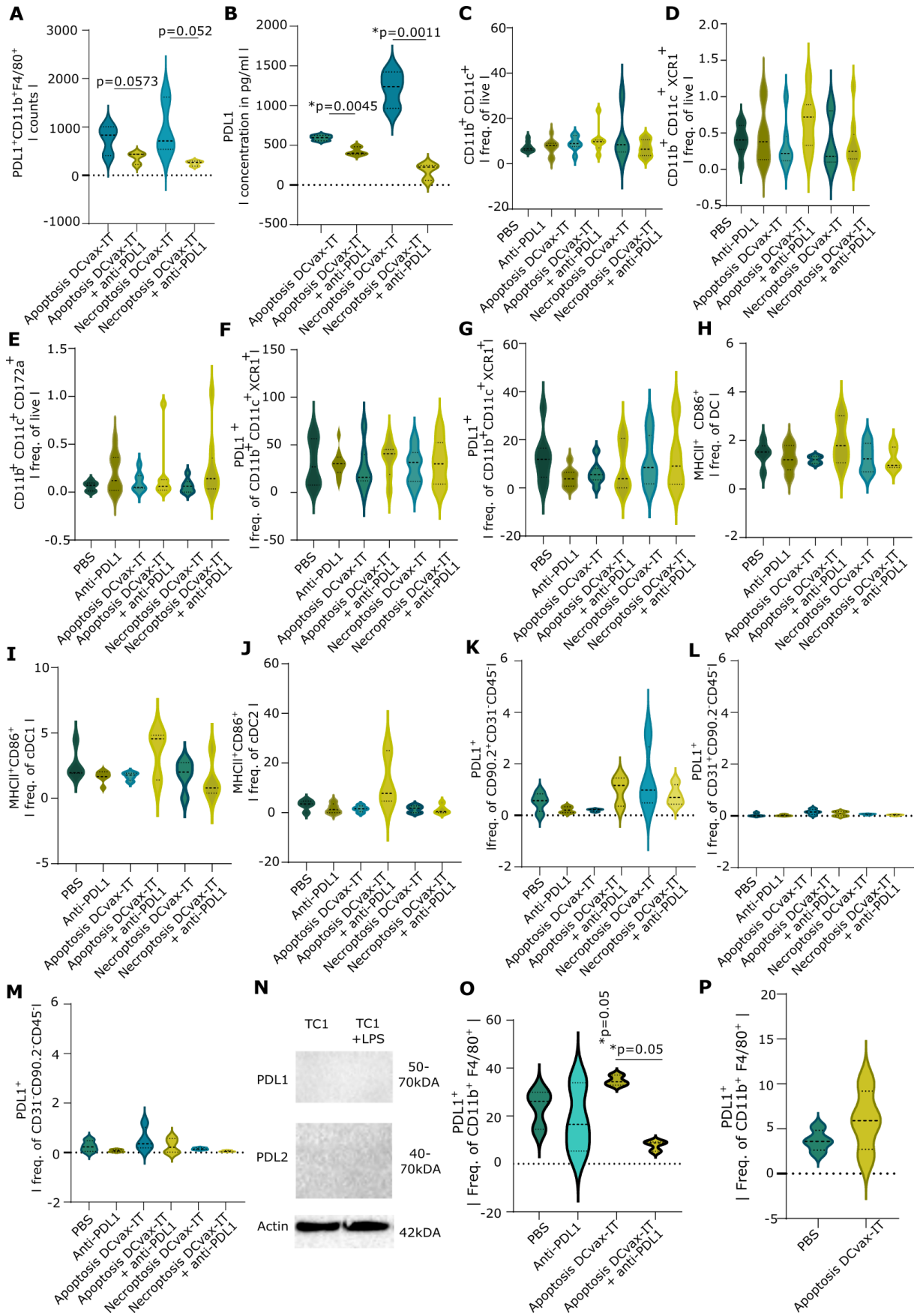


Figure S6, Phenotyping of the innate immune population of DC vaccinated tumours, related to Figure 6.

(A) Flow cytometry analysis of the CD45⁺ fraction from subcutaneous wild-type TC1 tumors isolated on day 23 after tumor cell injection, treated with DCvax-IT on day 9 and 16 and/or anti-PDL1 ICB on day 10 and 17. Violin plot of counts of PDL1⁺CD11b⁺ F4/80⁺ cells. (biological replicates; n=3; one-tailed unpaired t-test)

(B) PD-L1 concentration of the F4/80⁺ fraction from subcutaneous wild-type TC1 tumors isolated on day 23 after tumor cell injection, treated with DCvax-IT on day 9 and 16 and/or anti-PDL1 ICB on day 10 and 17. (biological replicates; n=3; one-tailed unpaired t-test)

(C-J) TIL analysis of the CD45⁺ fraction from wild-type TC1 tumor treated with DCvax-IT on day 9 and 16 and with anti-PDL1 on day 10 and 17, isolated on day 23 after wild-type TC1 cell injection. Violin plots of the frequency of (C) CD11b⁺CD11c⁺ of CD3⁻ cells (D) CD11b⁺CD11c⁺XCR1⁺ of CD3⁻ cells (E) CD11b⁺CD11c⁺CD172a⁺ of CD3⁻ cells (F) PDL1⁺ of CD11b⁺ CD11c⁺XCR1⁺ cells (G) PDL1⁺ of CD11b⁺ CD11c⁺CD172a⁺ cells (H) MHCII⁺CD86⁺ of CD11b⁺ CD11c⁺ cells (I) MHCII⁺CD86⁺ of CD11b⁺ CD11c⁺XCR1⁺ cells (J) MHCII⁺CD8 of CD11b⁺ CD11c⁺CD172a⁺ cells. Comparison to PBS treated mice (biological replicates; n=4-9; Mann-Whitney test).

(K-M) Flow cytometry analysis of the CD45⁻ fraction from wild-type TC1 tumor treated with DCvax-IT on day 9 and 16 and with anti-PD-L1 ICB on day 10 and 17, isolated on day 23 after wild-type TC1 cell injection. Violin plots of the frequency of (K) PDL1⁺ cells of CD90.2⁺CD31⁻CD45⁻ (L) PDL1⁺ cells of CD31⁺CD90.2⁻CD45⁻ (M) PDL1⁺ cells of CD31⁻CD90.2⁻CD45⁻. Comparison to PBS treated mice (biological replicates; n=3-4; one-way ANOVA).

(N) Western blot analysis for PD-L1 and PD-L2 of TC1 untreated and treated with LPS.

(O) Flow cytometry TIL analysis of the CD45⁺ fraction from subcutaneous wild-type LLC tumors isolated on day 23 after tumor cell injection, treated with DCvax-IT on day 9 and 16 and/or anti-PD-L1 ICB on day 10 and 17. Violin plot of frequency of PD-L1⁺ cells of CD11b⁺ F4/80⁺ cells. (biological replicates; n=3; one-tailed Mann-Whitney test)

(P) Flow cytometry TIL analysis of the CD45⁺ fraction from subcutaneous wild-type MC38 tumors isolated on day 23 after tumor cell injection, treated with DCvax-IT on day 9 and 16. Violin plot of frequency of PD-L1⁺ cells of CD11b⁺ F4/80⁺ cells. (biological replicates; n=4; unpaired t test)

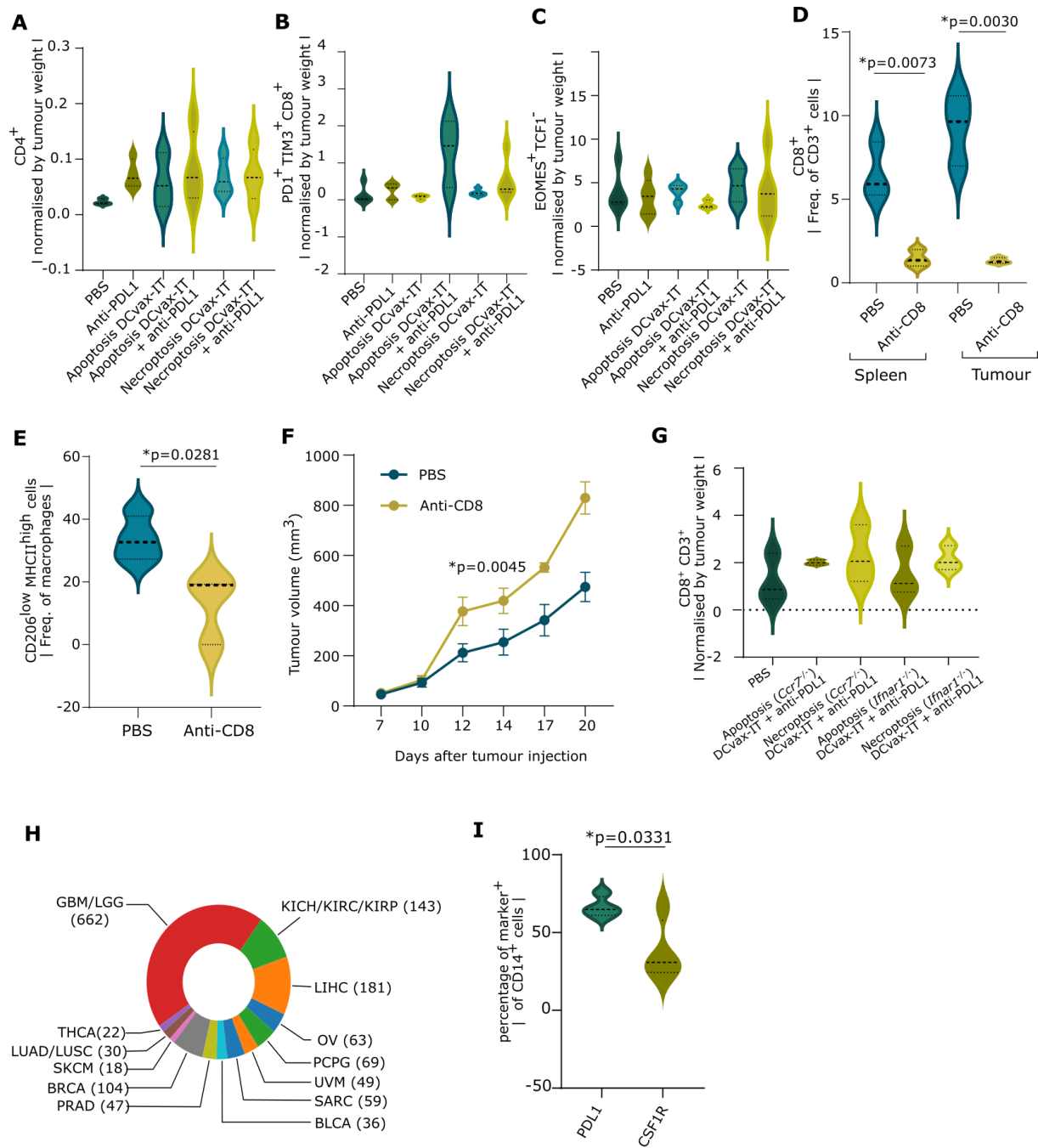


Figure S7, Analysis of adaptive immune population of DC vaccinated murine tumours and TCGA classification, related to Figure 6 and 7.

(A-C) TIL analysis of the CD45⁺ fraction from wild-type TC1 tumor treated with DCvax-IT on day 9 and 17 with or without anti-PDL1 injection on day 10 and 17 normalized by tumor weight at day of isolation. Frequency of (A) CD4⁺ of CD3⁺ (B) PD1⁺TIM3⁺ of CD8⁺ cells (C) EOMES⁺ TCF1⁻ of CD8⁺ cells. Comparison to PBS treated mice (biological replicates; n=3-5; Mann-Whitney test).

(D) Frequency of CD8⁺ of CD3⁺ cells in the CD45⁺ cell fraction of tumors isolated on day 23 after TC injection or spleen of untreated and anti-CD8 treated wild-type TC1 tumor bearing mice. P-values depict comparison to PBS treated mice (biological replicates; n=3; two-tailed student's t test).

(E) Frequency of CD206^{low}MHCII^{high} in the CD45⁺ cell fraction of tumors isolated on day 23 after TC injection of untreated and anti-CD8 treated wild-type TC1 tumors. (biological replicates; n=3; two-tailed student's t test).

(F) Tumor volume of untreated and anti-CD8 treated wild-type TC1 tumors. (biological replicates; n=3; area under curve; two-tailed student's t test).

(G) TIL analysis of the CD45⁺ fraction isolated from wild-type TC1 tumor on day 23 after tumor injection. Tumors were treated with *Ifnar1*^{-/-} or *Ccr7*^{-/-} DCvax-it on day 9 and 16 in combination with anti-PDL1 injection on day 10 and 17. Frequency of CD8⁺ of CD3⁺ cells. Comparison to PBS treated mice. (biological replicates; n=3; One-way ANOVA, Kruskal-Wallis test)

(H) Cancer-type distribution analyses amongst all the TCGA C4/C5-tumours. (biological replicates; glioblastoma/low grade glioma GBM; n=622, kidney chromophobe/kidney renal clear cell carcinoma/kidney renal papillary cell carcinoma KICH/KIRC/KIRP; n=143, liver hepatocellular carcinoma LIHC; n=181, ovarian serous cystadenocarcinoma OV; n=63, pheochromocytoma PCPG; n=69, uveal melanoma UVM; n=49, sarcoma SARC; n=59, Bladder urothelial carcinoma BLCA; n=36, prostate adenocarcinoma PRAD; n=47, breast invasive carcinoma BRCA; n=104, skin cutaneous melanoma SKCM; n=18, lung adenocarcinoma/lung squamous cell carcinoma LUAD/LUSC; n=30, thyroid carcinoma THCA; n=22

(I) Frequency of PDL1⁺ or CSF1R⁺ of CD14⁺ macrophages isolated from glioblastoma tumor samples obtained on the day of resection at first diagnosis. (biological replicates; n=4; two-tailed student's t test).